Mon. Not. R. Astron. Soc. **368,** 371–378 (2006) doi:10.1111/j.1365-2966.2006.10108.x

Constraining the cosmological parameters and transition redshift with gamma-ray bursts and supernovae

F. Y. Wang and Z. G. Dai★
Department of Astronomy, Nanjing University, Nanjing 210093, China

Accepted 2006 January 27. Received 2006 January 26; in original form 2005 November 21

ABSTRACT

A new method of measuring cosmology with gamma-ray bursts (GRBs) has been proposed by Liang and Zhang recently. In this method, only observable quantities including the rest-frame peak energy of the νF_ν spectrum ($E'_{\rm p}$), the isotropic energy of GRB ($E_{\gamma,\rm iso}$) and the break time of the optical afterglow light curves in the rest frame ($t'_{\rm b}$) are used. By considering this method, we constrain the cosmological parameters and the redshift at which the Universe expanded from the deceleration to acceleration phase. We add five recently detected GRBs to the sample and derive $E_{\gamma,\rm iso}/10^{52}\,{\rm erg} = (0.93 \pm 0.25)\,(E'_{\rm p}/100\,{\rm keV})^{1.91\pm0.32}(t'_{\rm b}/1\,{\rm d})^{-0.93\pm0.38}$ for a flat universe with $\Omega_{\rm M} = 0.28$ and $H_0 = 71.0\,{\rm km\,s^{-1}\,Mpc^{-1}}$. This relation is independent of the medium density around bursts and the efficiency of conversion of the explosion energy to gamma-ray energy. We consider the $E_{\gamma,\rm iso}(E'_{\rm p},\,t'_{\rm b})$ relationship as a standard candle and find $0.05 < \Omega_{\rm M} < 0.48$ and $\Omega_\Lambda < 1.15$ (at the 1σ confidence level). In a flat universe with the cosmological constant, we obtain $0.25 < \Omega_{\rm M} < 0.46$ and $0.54 < \Omega_\Lambda < 0.78$ at the 1σ confidence level. The transition redshift is $z_{\rm T} = 0.69^{+0.11}_{-0.12}$. Combining 20 GRBs with 157 Type Ia supernovae (SNe Ia), we find $\Omega_{\rm M} = 0.29 \pm 0.03$ for a flat universe and the transition redshift is $z_{\rm T} = 0.61^{+0.06}_{-0.05}$, which is slightly larger than the value found by considering SNe Ia alone. In particular, we also discuss several dark-energy models in which the equation of state $w(z)$ is parametrized, and investigate constraints on the cosmological parameters in detail.

Key words: supernovae: general – cosmology: observations – distance scale – gamma-rays: bursts.

1 INTRODUCTION

The property of dark energy and the physical cause of acceleration of the present Universe are two of the most difficult problems in modern cosmology. In the past several years, many authors used distant Type Ia supernovae (SNe Ia: Riess et al. 1998, 2004; Perlmutter et al. 1999), cosmic microwave background (CMB) fluctuations (Bennett et al. 2003; Spergel et al. 2003) and large-scale structure (LSS: Tegmark et al. 2004) to explore cosmology. Very recently, there have been extensive discussions on using gamma-ray bursts (GRBs) to constrain cosmological parameters (Dai, Liang & Xu 2004; Ghirlanda et al. 2004a; Di Girolamo et al. 2005; Firmani et al. 2005; Friedmann & Bloom 2005; Lamb et al. 2005; Liang & Zhang 2005; Mortsell & Sollerman 2005; Xu, Dai & Liang 2005).

SNe Ia have been considered as astronomical standard candles and used to measure the geometry and dynamics of the Universe. Phillips (1993) found the intrinsic relation in SNe Ia: $L_{\rm p} = a\triangle m_{15}^{\rm b}$, where $L_{\rm p}$ is the peak luminosity and $\triangle m_{15}$ is the decline rate in the optical band at day 15 after the peak. This relation and other similar relations can be used to explore cosmology. Riess et al. (1998) considered 16 high-redshift supernovae and 34 nearby supernovae and found that our present Universe has been accelerating. Perlmutter et al. (1999) used 42 SNe Ia and drew the same conclusion. Riess et al. (2004) selected 157 well-measured SNe Ia, which is called the 'gold' sample. Assuming a flat universe, they concluded that (1) using the strong prior of $\Omega_{\rm M} = 0.27 \pm 0.04$, fitting a static dark-energy equation of state yields $-1.46 < w < -0.78$ (95 per cent confidence level); (2) assuming a possible redshift dependence of $w(z)$ (using $w(z) = w_0 + w_1 z$), the data with the strong prior indicate that the region $w_1 < 0$ and especially the quadrant ($w_0 > -1$ and $w_1 < 0$) are the least favoured; and (3) $q(z)$ expands into two terms: $q(z) = q_0 + z{\rm d}q/{\rm d}z$. If the transition redshift is defined through $q(z_{\rm T}) = 0$, they found $z_{\rm T} = 0.46 \pm 0.13$. The cosmological use of SNe Ia has the following advantages: the SN Ia sample is very large and includes low-z sources, so the parameters a and b can be calibrated by using low-z SNe Ia. The Phillips relation and other similar relations are intrinsic and cosmology-independent, so that they can be used to explore cosmology. But they also have disadvantages: the interstellar medium extinction may exist when optical photons propagate

★E-mail: dzg@nju.edu.cn

towards us. In addition, the maximum redshift of SNe Ia is only about 1.7 and thus the earlier Universe may not be well studied. Higher-redshift SNe Ia are necessary to eliminate parameter degeneracies in studying the evolution of dark energy (Weller & Albrecht 2002; Linder & Huterer 2003).

GRBs are the most intense electromagnetic explosions in the Universe after the big bang. They have been well understood since the discovery of afterglows in 1997 (for review articles, see Piran 1999, 2004; van Paradijs, Kouveliotou & Wijers 2000; Mészáros 2002; Zhang & Mészáros 2004). It has been widely believed that they should be detectable out to very high redshifts (Ciardi & Loeb 2000; Lamb & Reichart 2000; Bromm & Loeb 2002; Gou et al. 2004). Schaefer (2003) derived the luminosity distances of nine GRBs with known redshifts by using two quantities (the spectral lag and the variability). He obtained the first GRB Hubble diagram with the mass density $\Omega_{\rm M} < 0.35$ (at the 1σ confidence level). Ghirlanda, Ghisellini & Lazzati (2004b) found the relation between isotropic-equivalent energy $E_{\gamma,\rm iso}$ and the local-observer peak energy $E'_{\rm p}$ (i.e. the Ghirlanda relation). Unfortunately, because of the absence of low-z GRBs, the Ghirlanda relation has been obtained only from moderate-z GRBs. So this relation is cosmology-dependent. Dai et al. (2004) used for the first time the Ghirlanda relation with 12 bursts and found the mass density $\Omega_{\rm M} = 0.35 \pm 0.15$ (at the 1σ confidence level) for a flat universe with the cosmological constant and the w parameter of the static dark-energy model $-1.27 < w < -0.50$ (1σ). Combining 14 GRBs with SNe Ia, Ghirlanda et al. (2004b) obtained $\Omega_{\rm M} = 0.37 \pm 0.10$ and $\Omega_\Lambda = 0.87 \pm 0.23$. Assuming a flat universe, the cosmological parameters were constrained: $\Omega_{\rm M} = 0.29 \pm 0.04$ and $\Omega_\Lambda = 0.71 \pm 0.05$. Firmani et al. (2005) used the Bayesian method to solve the circularity problem. For a flat universe, they found $\Omega_{\rm M} = 0.28 \pm 0.03$ and $z_{\rm T} = 0.73 \pm 0.09$ for the combined GRB+SN Ia sample. In the dark-energy model of $w_z = w_0$, they found $\Omega_{\rm M} = 0.44$ and $w_0 = -1.68$ with $z_{\rm T} = 0.40$ for the combined GRB+SN Ia sample. In the dark-energy model of $w_z = w_0 + w_1 z$, they found the best values for GRB+SN Ia sample were $w_0 = -1.19$ and $w_1 = 0.98$ with $z_{\rm T} = 0.55$. Xu et al. (2005) obtained $\Omega_{\rm M} = 0.15^{+0.45}_{-0.13}$ (1σ) using 17 GRBs. Friedmann & Bloom (2005) discussed several possible sources of systematic errors in using GRBs as standard candles. Liang & Zhang (2005) presented a multivariable regression analysis to three observable quantities for a sample of 15 GRBs without assumption of any theoretical models. They obtained a relation among the isotropic gamma-ray energy ($E_{\gamma,\rm iso}$), the peak energy of the νF_ν spectrum in the rest frame ($E'_{\rm p}$) and the rest-frame break time of the optical afterglow light curves ($t'_{\rm b}$). Using this relation, they found the 1σ constraints are $0.13 < \Omega_{\rm M} < 0.49$ and $0.50 < \Omega_\Lambda < 0.85$ for a flat universe. They also obtained the transition redshift $0.78^{+0.32}_{-0.23}$ (1σ). Ghirlanda et al. (2005) used their relation in a homogeneous density profile and a wind density profile to explore cosmology. Liang & Zhang (2006) proposed an approach to calibrate the GRB luminosity indicators without introduction of a low-redshift GRB sample. The cosmological use of GRBs has following advantages. First, gamma-ray photons suffer from no extinction when they propagate towards us. Secondly, GRBs are likely to occur at high redshifts. We can thus study the early Universe. Recently, GRB 050904, which has a redshift of 6.29, was detected (Haislip et al. 2005; Kawai et al. 2005). But the low-z GRB sample is so small that the intrinsic relation cannot be obtained. A cosmology-dependent relation is now used to constrain the cosmological parameters and transition redshift.

In this paper, we investigate cosmological constraints and the transition redshift following the method of Liang & Zhang (2005). Our GRB sample contains 20 bursts. Combining this sample with 157 SNe Ia, we constrain the cosmological parameters and the transition redshift in several dark-energy models in detail. The structure of this paper is arranged as follows. In Section 2, we list our sample and results from the regression analysis. In Section 3, we explore the constraints on cosmological parameters and transition redshift using the GRB and SN Ia sample in different dark-energy models. In Section 4, we present conclusions and a brief discussion.

2 THE METHOD

2.1 Sample selection

Our sample includes 20 GRBs. We add GRBs 970828, 990705, 041006, 050408 and 050525a to the sample of Liang & Zhang (2005). The redshift z, spectral peak energy $E_{\rm p}$ and optical break time $t_{\rm b}$ of these bursts have been well measured. The uncertainties of $E_{\rm p}$, S_γ and k-correction of some bursts have not been reported. They are taken to be 20, 10 and 5 per cent of the values. Our GRB sample is listed in Table 1.

2.2 Cosmology with the cosmological constant

The isotropic-equivalent gamma-ray energy of a GRB is calculated by

$$E_{\gamma,\rm iso} = \frac{4\pi D_{\rm L}^2(z) S_\gamma k}{1+z}, \tag{1}$$

where $D_{\rm L}(z)$ is the luminosity distance at redshift z, and k is the factor that corrects the observed fluence to the standard rest-frame bandpass (1–10^4 keV; Bloom, Frail & Sari 2001). The expression of $D_{\rm L}(z)$ is different in different dark-energy models. In a Friedmann–Robertson–Walker (FRW) cosmology with mass density $\Omega_{\rm M}$ and vacuum energy density Ω_Λ, the luminosity distance in equation (1) is

$$D_{\rm L}(z) = c(1+z)H_0^{-1}|\Omega_k|^{-1/2}{\rm sinn}\left\{|\Omega_k|^{1/2} \times \int_0^z {\rm d}z\left[(1+z)^2(1+\Omega_{\rm M}z) - z(2+z)\Omega_\Lambda\right]^{-1/2}\right\}, \tag{2}$$

where c is the speed of light and $H_0 \equiv 100\,h\,{\rm km\,s^{-1}\,Mpc^{-1}}$ is the present Hubble constant (Carroll, Press & Turner 1992). In equation (2), $\Omega_k = 1 - \Omega_{\rm M} - \Omega_\Lambda$, and 'sinn' is sinh for $\Omega_k > 0$ and sin for $\Omega_k < 0$. For $\Omega_k = 0$, equation (2) turns out to be $c(1+z)H_0^{-1}$ times the integral. In this model, the transition redshift satisfies

$$z_{\rm T} = \left(\frac{2\Omega_\Lambda}{\Omega_{\rm M}}\right)^{1/3} - 1. \tag{3}$$

2.3 One-parameter dark-energy model

We consider an equation of state for dark energy

$$w_z = w_0. \tag{4}$$

In this dark-energy model, the luminosity distance for a flat universe is (Riess et al. 2004)

$$D_{\rm L} = cH_0^{-1}(1+z)\int_0^z {\rm d}z\left[(1+z)^3\Omega_{\rm M} + (1-\Omega_{\rm M})(1+z)^{3(1+w_0)}\right]^{-1/2}. \tag{5}$$

The transition redshift satisfies

$$\Omega_{\rm M} + (1-\Omega_{\rm M})(1+3w_0)(1+z)^{3w_0} = 0. \tag{6}$$

Table 1. The parameters of the GRB sample used in this paper.

GRB (1)	z (2)	$E_{\rm p}(\sigma_{E_{\rm p}})$ (keV) (3)	α (4)	β (5)	$S_\gamma(\sigma_S)$ (erg cm^{-2}) (6)	Band (keV) (7)	$t_{\rm b}(\sigma_{t_{\rm b}})$ (d) (8)	Refs. (9)
970828	0.9578	297.7(59.5)	−0.70	−2.07	96.0(9.6)	20–2000	2.2(0.4)	1; 5; 20; 20
980703	0.966	254(50.8)	−1.31	−2.40	22.6(2.3)	20–2000	3.4(0.5)	2; 3; 3; 3
990123	1.6	780.8(61.9)	−0.89	−2.45	300(40)	40–700	2.04(0.46)	4; 5; 5; 5
990510	1.62	161.5(16.1)	−1.23	−2.70	19(2)	40–700	1.6(0.2)	6; 5; 5; 5
990705	0.8424	188.8(15.2)	−1.05	−2.20	75.0(8.0)	40–700	1.0(0.2)	1; 19; 20; 20
990712	0.43	65(11)	−1.88	−2.48	6.5(0.3)	40–700	1.6(0.2)	6; 5; 5; 5
991216	1.02	317.3(63.4)	−1.23	−2.18	194(19)	20–2000	1.2(0.4)	7; 3; 3; 3
011211	2.14	59.2(7.6)	−0.84	−2.30	5.0(0.5)	40–700	1.56(0.02)	8; 9; 9; 8
020124	3.2	86.9(15.0)	−0.79	−2.30	8.1(0.8)	2–400	3(0.4)	10; 11; 11; 11
020405	0.69	192.5(53.8)	0.00	−1.87	74.0(0.7)	15–2000	1.67(0.52)	12; 12; 12; 12
020813	1.25	142(13)	−0.94	−1.57	97.9(10)	2–400	0.43(0.06)	13; 11; 11; 11
021004	2.332	79.8(30)	−1.01	−2.30	2.6(0.6)	2–400	4.74(0.14)	14; 11; 11; 11
021211	1.006	46.8(5.5)	−0.86	−2.18	3.5(0.1)	2–400	1.4(0.5)	15; 11; 11; 11
030226	1.986	97(20)	−0.89	−2.30	5.61(0.65)	2–400	1.04(0.12)	16; 11; 11; 11
030328	1.52	126.3(13.5)	−1.14	−2.09	37.0(1.4)	2–400	0.8(0.1)	17; 11; 11; 11
030329	0.1685	67.9(2.2)	−1.26	−2.28	163(10)	2–400	0.5(0.1)	18; 11; 11; 11
030429	2.6564	35(9)	−1.12	−2.30	0.85(0.14)	2–400	1.77(1)	19; 11; 11; 11
041006	0.716	63.4(12.7)	−1.37	−2.30	19.9(1.99)	25–100	0.16(0.04)	20; 20; 21; 21
050408	1.2357	19.93(4.0)	−1.979	−2.30	1.90(0.19)	30–400	0.28(0.17)	22; 22; 23; 23
050525a	0.606	79.0(3.5)	−0.987	−8.839	20.1(0.50)	15–350	0.28(0.12)	24; 24; 24; 24

References are in order for z, $E_{\rm p}^{\rm obs}$, [α, β], S_γ, $t_{\rm b}$: (1) Bloom, Morrell & Mohanty 2003; (2) Djorgovski et al. (1998); (3) Jimenez, Band & Piran (2001); (4) Kulkarni et al. (1999); (5) Amati et al. (2002); (6) Vreeswijk et al. (2001); (7) Djorgovski et al. 1999; (8) Holland et al. (2002); (9) Amati (2004); (10) Hjorth et al. (2003); (11) Sakamoto et al. 2005a; (12) Price et al. (2003); (13) Barth et al. (2003); (14) Möller et al. (2002); (15) Vreeswijk et al. (2003); (16) Greiner et al. (2003); (17) Martini, Garnavich & Stanek (2003); (18) Bloom et al. 2004; (19) Weidinger et al. (2003); (20) Butler et al. 2005; (21) Stanek et al. (2005); (22) Sakamoto et al. 2005; (23) Godet et al. (2005); (24)Blustin et al. (2006).

2.4 Two-parameter dark-energy model

A more interesting approach to explore dark energy is to use a time-dependent dark-energy model. The simplest parametrization including two parameters is (Maor, Brustein & Steinhardt 2001; Weller & Albrecht 2001, 2002; Riess et al. 2004)

$$w_z = w_0 + w_1 z. \tag{7}$$

This parametrization provides the minimum possible resolving power to distinguish between the cosmological constant and a rolling scalar field from the time variation. The value of w_1 could provide an estimate of the scalelength of a dark-energy potential (Riess et al. 2004). In this dark-energy model,the luminosity distance is (Linder 2003)

$$D_{\rm L} = cH_0^{-1}(1+z)\int_0^z {\rm d}z\Big[(1+z)^3\Omega_{\rm M} + (1-\Omega_{\rm M})(1+z)^{3(1+w_0-w_1)}{\rm e}^{3w_1 z}\Big]^{-1/2}. \tag{8}$$

The transition redshift is given by

$$\Omega_{\rm M} + (1-\Omega_{\rm M})(1+3w_0+3w_1 z)(1+z)^{w_0-w_1}{\rm e}^{3w_1 z} = 0. \tag{9}$$

The above model is incompatible with the CMB data since it diverges at high redshifts (Chevallier & Polarski 2001). Linder (2003) proposed an extended parametrization which avoids this problem,

$$w_z = w_0 + \frac{w_1 z}{1+z}. \tag{10}$$

We adopt the results only if $w_0 + w_1$ is well below zero at the time of decoupling. In this dark-energy model, the luminosity distance is

$$D_{\rm L} = cH_0^{-1}(1+z)\int_0^z {\rm d}z\,\Big[(1+z)^3\Omega_{\rm M} + (1-\Omega_{\rm M})(1+z)^{3(1+w_0+w_1)}{\rm e}^{-3w_1 z/(1+z)}\Big]^{-1/2}. \tag{11}$$

The transition redshift is given by

$$\Omega_{\rm M} + (1-\Omega_{\rm M})\left(1+3w_0+\frac{3w_1 z}{1+z}\right) \times (1+z)^{w_0+w_1}{\rm e}^{-3w_1 z/(1+z)} = 0. \tag{12}$$

By fitting the SN Ia data using the $w_z = w_0 + (w_1 z)/(1+z)$ model, $w_0 + w_1 > 0$ was found and thus at high redshifts this model is not good. In order to solve this problem, Jassal, Bagla and Padmanabhan modified this parametrization as

$$w_z = w_0 + \frac{w_1 z}{(1+z)^2}. \tag{13}$$

This equation can model a dark-energy component that has the same value at lower and higher redshifts, with rapid variation at low z. Observations are not very sensitive to variations in w_z for $z \gg 1$. However, it does allow us to probe rapid variations at small redshifts (Jassal, Bagla & Padmanabhan 2004). The luminosity distance in this dark-energy model is

$$D_{\rm L} = cH_0^{-1}(1+z)\int_0^z {\rm d}z\,\Big[(1+z)^3\Omega_{\rm M} + (1-\Omega_{\rm M})(1+z)^{3(1+w_0)}{\rm e}^{3w_1 z^2/2(1+z)^2}\Big]^{-1/2}. \tag{14}$$

The transition redshift is given by

$$\Omega_{\rm M} + (1-\Omega_{\rm M})\left(1+3w_0+\frac{3w_1 z}{(1+z)^2}\right) \times (1+z)^{3w_0}{\rm e}^{3w_1 z^2/2(1+z)^2} = 0. \tag{15}$$

2.5 Regression analysis

We perform a three-variable regression analysis to find an empirical relation among $E_{\gamma,\rm iso}$, $E'_{\rm p}$ and $t'_{\rm b}$. The model that we use is

$$\hat{E}_{\rm iso} = 10^{\kappa_0} E_{\rm p}^{\prime\kappa_1} t_{\rm b}^{\prime\kappa_2}, \quad (16)$$

where $E'_{\rm p} = E_{\rm p}(1+z)$ and $t'_{\rm b} = t_{\rm b}/(1+z)$. For a flat universe with $\Omega_{\rm M} = 0.28$, using the sample of 20 GRBs, we find a relation among $E_{\gamma,\rm iso}$, $E'_{\rm p}$ and $t'_{\rm b}$,

$$\hat{E}_{\gamma,\rm iso,52} = (0.93 \pm 0.25) \left(\frac{E'_{\rm p}}{100\,\rm keV}\right)^{1.91\pm0.32} \times \left(\frac{t'_{\rm b}}{1\,\rm d}\right)^{-0.93\pm0.38}, \quad (17)$$

where $\hat{E}_{\gamma,\rm iso,52} = \hat{E}_{\gamma,\rm iso}/10^{52}$ erg. This relation depends on the cosmology that we choose. Fig. 1 shows that $E_{\gamma,\rm iso}$ strongly depends on both $E'_{\rm p}$ and $t'_{\rm b}$. The dispersion of this relation is so small that it can be used to study cosmology (Liang & Zhang 2005). We don't assume any theoretical models when deriving this relation. With $D_{\rm L}$ in units of megaparsecs, the distance modulus is

$$\hat{\mu} = 5\log(D_{\rm L}) + 25. \quad (18)$$

Thus,

$$\hat{\mu} = 2.5[\kappa_0 + \kappa_1 \log E'_{\rm p} + \kappa_2 \log t'_{\rm b} - \log(4\pi S_\gamma k) + \log(1+z)] - 97.45. \quad (19)$$

Because of the cosmology-dependent relation, $\hat{\mu}$ is cosmology-dependent. We need low-z GRBs to calibrate a cosmology-independent relation, but the current low-z GRBs sample is small.

We use the following method to solve this problem (also see Liang & Zhang 2005).

(i) Given a particular set of cosmological parameters ($\bar{\Omega}$), we calculate the correlation $\hat{E}_{\gamma,\rm iso}(\bar{\Omega}; E'_{\rm p}, t'_{\rm b})$. We evaluate the probability [$w(\bar{\Omega})$] of using this relation as a cosmology-independent luminosity indicator via χ^2 statistics, i.e.

$$\chi^2_w(\bar{\Omega}) = \sum_i^N \frac{\left[\log \hat{E}^i_{\gamma,\rm iso}(\bar{\Omega}) - \log E^i_{\gamma,\rm iso}(\bar{\Omega})\right]^2}{\sigma^2_{\log \hat{E}^i_{\gamma,\rm iso}}(\bar{\Omega})}. \quad (20)$$

The probability is

$$w(\bar{\Omega}) \propto {\rm e}^{-\chi^2_w(\bar{\Omega})/2}. \quad (21)$$

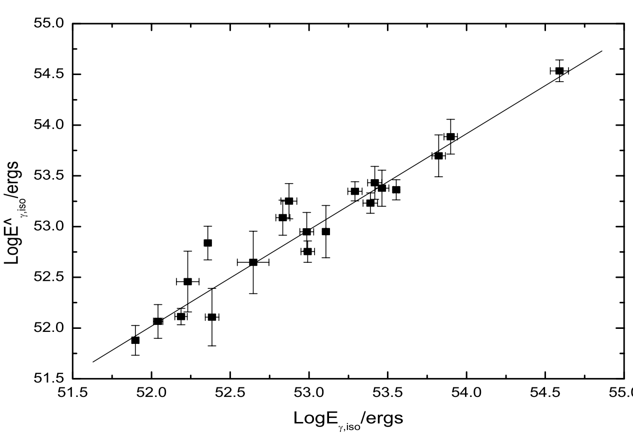

Figure 1. $\log \hat{E}_{\gamma,\rm iso}$ calculated by the regression method versus $\log E_{\gamma,\rm iso}$ calculated from a flat universe with $\Omega_{\rm M} = 0.28$. The line is the best regression line.

(ii) Regard the relation derived in step (1) as a cosmology-independent luminosity indicator without considering its systematic error, and calculate distance modulus $\hat{\mu}(\bar{\Omega})$ and its error $\sigma_{\hat{\mu}}$,

$$\sigma_{\hat{\mu}_i} = \frac{2.5}{\ln 10}\left[\left(\kappa_1 \frac{\sigma_{E'_{{\rm p},i}}}{E'_{{\rm p},i}}\right)^2 + \left(\kappa_2 \frac{\sigma_{t'_{{\rm b},i}}}{t'_{{\rm b},i}}\right)^2 + \left(\frac{\sigma_{S_{\gamma,i}}}{S_{\gamma,i}}\right)^2 + \left(\frac{\sigma_{k_i}}{k_i}\right)^2 + \left(\frac{\sigma_{z_i}}{1+z_i}\right)^2\right]^{1/2}. \quad (22)$$

(iii) Derive the theoretical distance modulus $\mu(\Omega)$ in a set of cosmological parameters, and the χ^2 of $\mu(\Omega)$ against $\hat{\mu}(\Omega)$,

$$\chi^2(\bar{\Omega}|\Omega) = \sum_i^N \frac{[\hat{\mu}_i(\bar{\Omega}) - \mu_i(\Omega)]^2}{\sigma^2_{\hat{\mu}_i}(\bar{\Omega})}. \quad (23)$$

(iv) Calculate the probability that the cosmology parameter set Ω is the right one according to the luminosity indicator derived from the cosmological parameter set $\bar{\Omega}$,

$$p(\bar{\Omega}|\Omega) \propto {\rm e}^{-\chi^2(\bar{\Omega}|\Omega)/2}. \quad (24)$$

(v) Integrate $\bar{\Omega}$ over the full cosmological parameter space to get the final normalized probability that the cosmological Ω is the right one,

$$p(\Omega) = \frac{\int_{\bar{\Omega}} w(\bar{\Omega}) p(\bar{\Omega}|\Omega)\,{\rm d}\bar{\Omega}}{\int_{\bar{\Omega}} w(\bar{\Omega}){\rm d}\bar{\Omega}}. \quad (25)$$

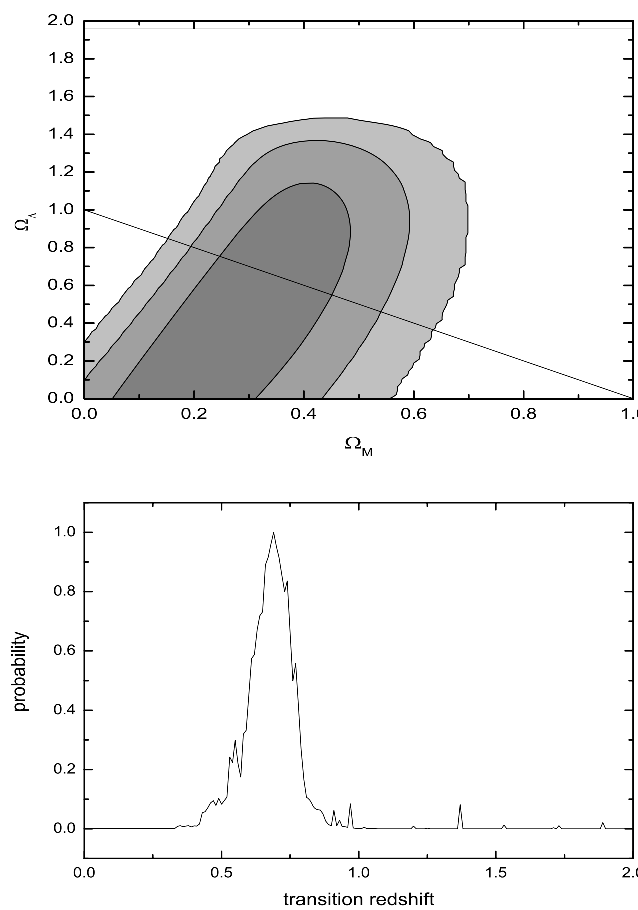

Figure 2. The top panel shows confidence interval distributions in the $\Omega_{\rm M}$–Ω_Λ plane from 1σ to 3σ in an FRW cosmology. The straight line represents a flat universe. The bottom panel shows the probability versus transition redshift.

In our calculation, the integration in equation (25) is computed through summing over a wide range of the cosmology parameter space to make the sum converge, i.e.

$$p(\Omega) = \frac{\sum_{\bar{\Omega}_i} w(\bar{\Omega}_i) p(\bar{\Omega}_i|\Omega)}{\sum_{\bar{\Omega}_i} w(\bar{\Omega}_i)}. \tag{26}$$

3 RESULTS

3.1 Cosmology with the cosmological constant

We obtain Fig. 2 in a FRW cosmology with mass density $\Omega_{\rm M}$ and vacuum energy density Ω_Λ using the GRB sample. This figure shows that $0.05 < \Omega_{\rm M} < 0.48$ at the 1σ confidence level, but Ω_Λ is poorly constrained: $\Omega_\Lambda < 1.15$. For a flat universe, we obtain $0.25 < \Omega_{\rm M} < 0.46$ and $0.54 < \Omega_\Lambda < 0.78$ at the 1σ confidence level. The best values of $(\Omega_{\rm M}, \Omega_\Lambda)$ are $(0.29, 0.62)$. The transition redshift at which the universe changed from the deceleration to acceleration phase is $z_{\rm T} = 0.69^{+0.11}_{-0.12}$ at the 1σ confidence level.

We plot Fig. 3 combining the GRB sample with the SN Ia sample. From this figure, we find $\Omega_{\rm M} = 0.29 \pm 0.03$ at the 1σ confidence level for a flat universe. The grey contours are derived from SNe Ia alone. The dashed contours are derived from the GRB and SNe Ia sample. We can see that the contours move down and become tighter as compared with the case of a combination of GRBs and SNe Ia. The result is more convincing than the one from SNe Ia alone. The transition redshift is $z_{\rm T} = 0.61^{+0.06}_{-0.05}$, which is slightly larger than the value found by considering SNe Ia alone. Fig. 4 shows the confidence level derived from SN Ia sample and eight $z > 1.5$ GRBs. The results are similar to those shown in Fig. 3. We

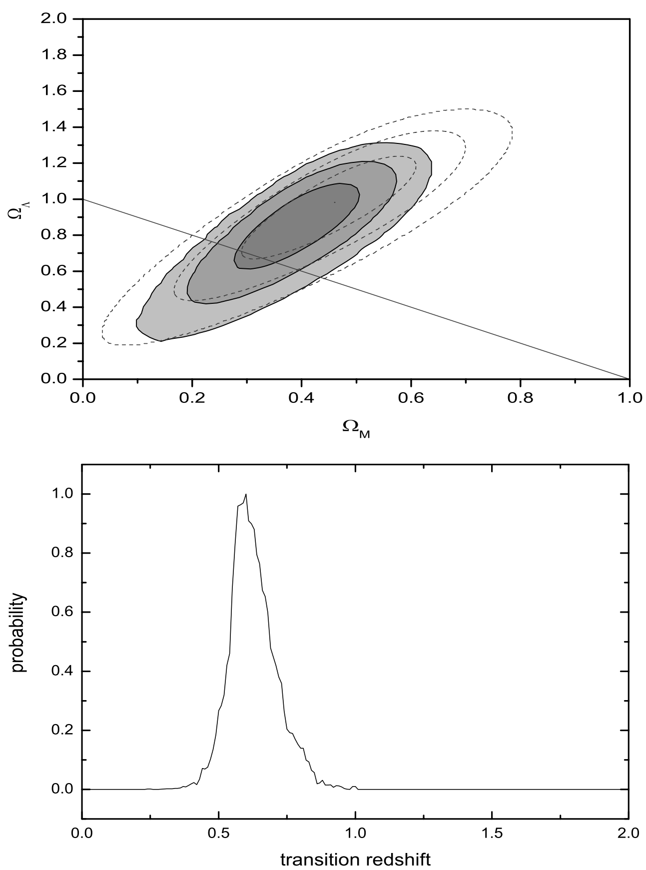

Figure 3. Constraints on $\Omega_{\rm M}$ and Ω_Λ from 1σ to 3σ in the top panel. The dashed contours are derived from 157 SNe Ia alone and the grey ones from the GRB and SN Ia sample. The bottom panel shows the probability versus the transition redshift derived from the GRB and SN Ia sample.

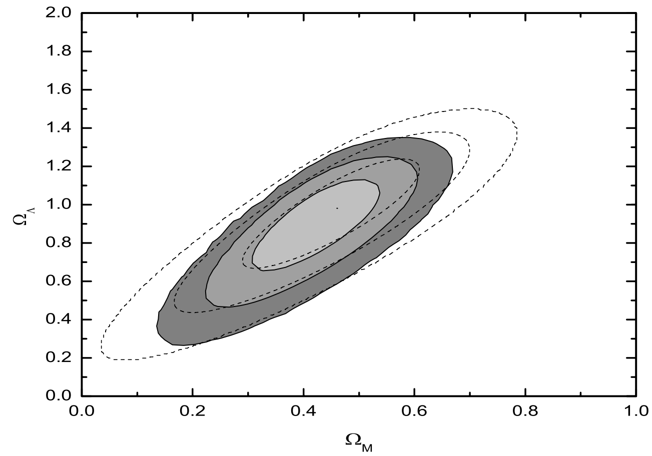

Figure 4. Constraints on $\Omega_{\rm M}$ and Ω_Λ from 1σ to 3σ derived from 157 SNe Ia and eight GRBs with redshifts greater than 1.5 (shown by grey contours). The dashed contours are derived from 157 SNe Ia alone.

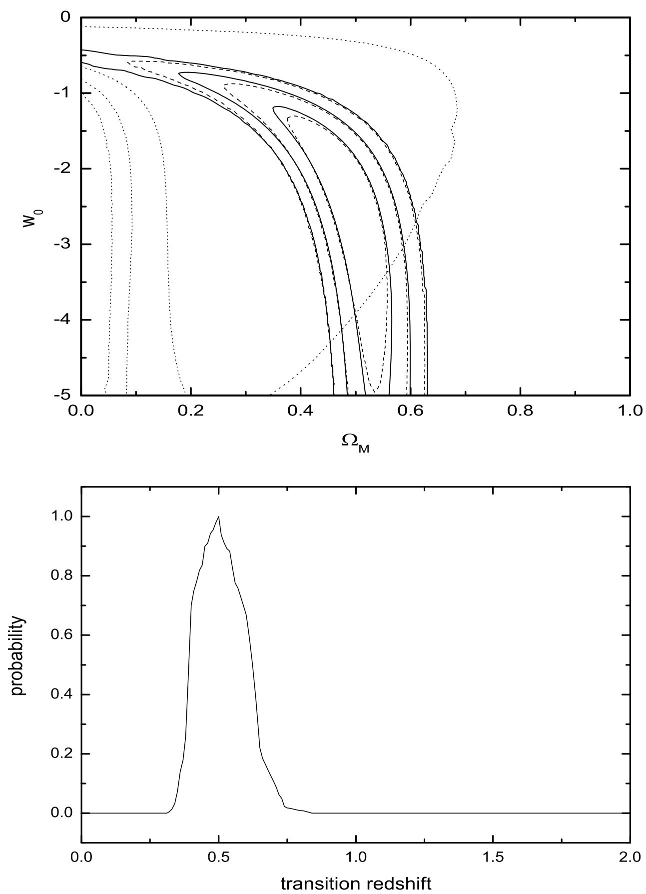

Figure 5. Constraints on $\Omega_{\rm M}$ and w_0 from 1σ to 3σ with dark energy whose equation state is constant in the top panel. The solid contours are derived from SNe Ia alone and the long-dashed contours are derived from 20 GRBs and Gold sample. The dotted contours are derived from 20 GRBs. The bottom panel shows the probability versus transition redshift derived from the GRB and SN Ia sample.

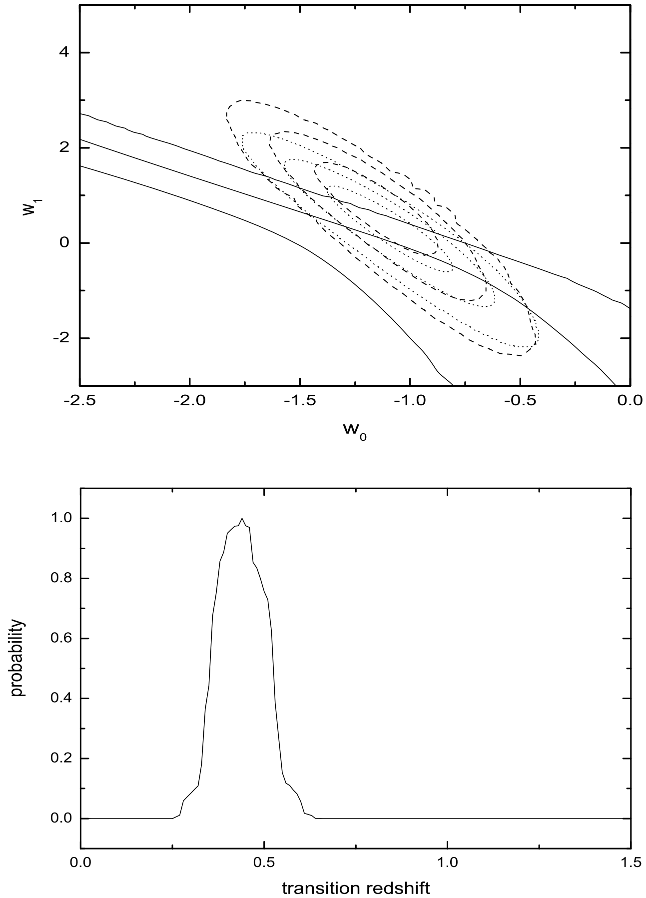

Figure 6. Constraints on w_0 and w_1 from 1σ to 3σ with dark energy whose equation state is $w_z = w_0 + w_1 z$ in the top panel. The long-dashed contours are derived from SNe Ia alone and the dotted contours are derived from 20 GRBs and Gold sample. The diagonal lines are obtained from 20 GRBs. The bottom panel shows the probability versus transition redshift derived from the GRB and SN Ia sample.

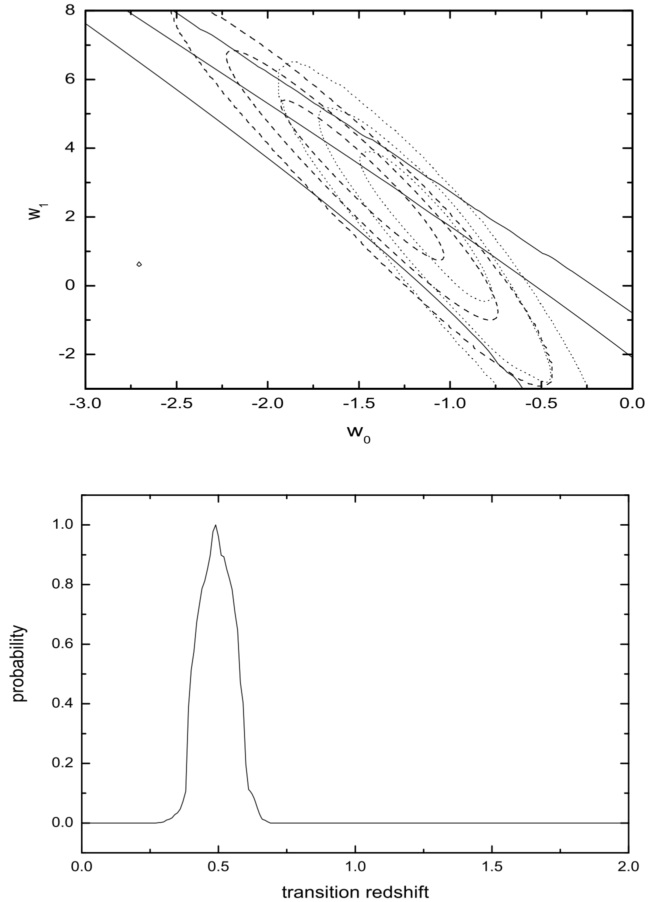

Figure 7. Constraints on w_0 and w_1 from 1σ to 3σ with dark energy whose equation state is $w_z = w_0 + w_1 z/(1+z)$ in the top panel. The long-dashed contours are derived from SNe Ia alone and the dotted contours are derived from 20 GRBs and Gold sample. The diagonal lines are obtained from 20 GRBs. The bottom panel shows the probability versus transition redshift derived from the GRB and SN Ia sample.

can conclude that an improvement of the confidence is due to the contribution of GRBs at moderate redshifts.

3.2 One-parameter dark-energy model

Fig. 5 shows the constraints on w_0 and $\Omega_{\rm M}$ in this dark-energy model. The best values for the SN Ia and GRB sample are $\Omega_{\rm M} = 0.48^{+0.07}_{-0.09}$ and $w_0 = -1.90^{+0.58}_{-2.85}$. The transition redshift is $z_{\rm T} = 0.50^{+0.09}_{-0.10}$. Riess et al. (2004) gave $w_0 = -1.02^{+0.13}_{-0.19}$ using SNe Ia sample with a prior of $\Omega_{\rm M} = 0.27 \pm 0.04$. Firmani et al. (2005) obtained $\Omega_{\rm M} = 0.44$ and $w_0 = -1.68$ from their SNe Ia and GRB sample using the Bayesian method.

3.3 Two-parameter dark-energy model

Fig. 6 exhibits the constraints on the dark-energy parameters (w_0 and w_1) and transition redshift in the model of $w_z = w_0 + w_1 z$. For the SN Ia and GRB sample, the best values are $w_0 = -1.20^{+0.18}_{-0.24}$ and $w_1 = 0.85^{+0.30}_{-0.25}$ with $z_{\rm T} = 0.44^{+0.09}_{-0.08}$ at the 1σ confidence level. Firmani et al. (2005) obtained $w_0 = -1.19$ and $w_1 = 0.98$ with $z_{\rm T} = 0.55$ using their SN Ia and GRB sample. From this figure, we see that the contours plotted from the SN Ia and GRB sample move down and become tighter.

Fig. 7 presents the constraints on the dark-energy parameters (w_0 and w_1) and transition redshift in the model of $w_z = w_0 + w_1 z/(1+z)$. The best values for the SN Ia and GRB sample are $w_0 = -1.12^{+0.32}_{-0.30}$ and $w_1 = 1.90^{+2.10}_{-1.75}$ (at the 1σ confidence level) with $z_{\rm T} = 0.49^{+0.07}_{-0.09}$. From this figure, we can also see that the contours plotted from the SN Ia and GRB sample move down and become tighter, being similar to Fig. 4.

Fig. 8 shows the constraints on the dark-energy parameters (w_0 and w_1) and transition redshift in the model of $w_z = w_0 + w_1 z/(1+z)^2$. The best values for the SN Ia and GRB sample are $w_0 = -1.00^{+0.22}_{-0.25}$ and $w_1 = 0.54^{+0.85}_{-1.20}$ with $z_{\rm T} = 0.37^{+0.10}_{-0.07}$ at the 1σ confidence level.

4 CONCLUSIONS AND DISCUSSION

Following Liang & Zhang (2005), we have derived an empirical relation among the rest-frame peak energy of the νF_ν spectrum ($E'_{\rm p}$), the isotropic energy of GRB ($E_{\gamma,rmiso}$) and the break time of the optical afterglow light curves in the rest frame ($t'_{\rm b}$) without any theoretical assumptions. The relation is $E_{\gamma,{\rm iso}}/10^{52}\,{\rm erg} = (0.93 \pm 0.25)\,(E'_{\rm p}/100\,{\rm keV})^{1.91\pm0.32}(t'_{\rm b}/1\,{\rm d})^{-0.93\pm0.38}$ in a flat universe with $\Omega_{\rm M} = 0.28$ and $H_0 = 71.0\,{\rm km\,s^{-1}\,Mpc^{-1}}$ for our sample with 20 GRBs. We find $0.05 < \Omega_{\rm M} < 0.48$ and $\Omega_\Lambda < 1.15$ (1σ). For a flat

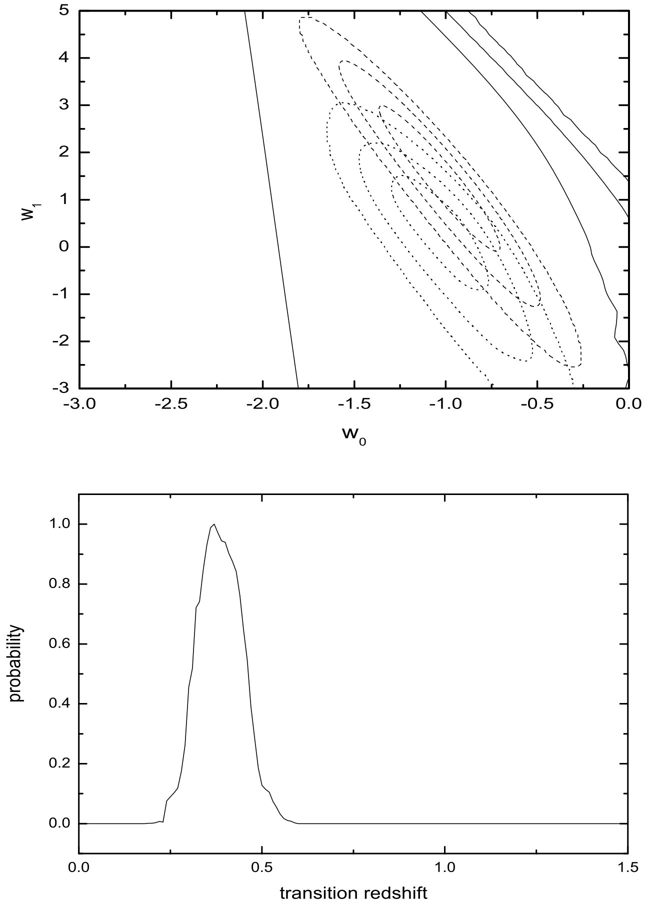

Figure 8. Constraints on w_0 and w_1 from 1σ to 3σ with dark energy whose equation state is $w_z = w_0 + w_1 z/(1+z)^2$ in the top panel. The long dashed contours are derived from SNe Ia alone and the dotted contours are derived from 20 GRBs and Gold sample. The diagonal lines are obtained from 20 GRBs. The bottom panel shows the probability versus transition redshift derived from the GRB and SN Ia sample.

universe with the cosmological constant, we obtain $0.25 < \Omega_{\mathrm{M}} < 0.46$ and $0.54 < \Omega_\Lambda < 0.78$ at the 1σ confidence level. The transition redshift is $z_{\mathrm{T}} = 0.69^{+0.11}_{-0.12}$. Because of the small number of useful GRBs, we combine GRBs with SNe Ia. Using this joint sample, we find $\Omega_{\mathrm{M}} = 0.29 \pm 0.03$ for a flat universe. The transition redshift is $z_{\mathrm{T}} = 0.61^{+0.06}_{-0.05}$, which is slightly larger than the value found by considering SN Ia alone. The best values for Ω_{M} and w_0 are $\Omega_{\mathrm{M}} = 0.48$ and $w_0 = -1.90$ with the GRB and SN Ia sample in the $w_z = w_0$ model. The transition redshift is $z_{\mathrm{T}} = 0.50^{+0.09}_{-0.10}$. For the SN Ia and GRB sample, the best values are $w_0 = -1.20^{+0.18}_{-0.24}$ and $w_1 = 0.85^{+0.30}_{-0.25}$ with $z_{\mathrm{T}} = 0.44^{+0.09}_{-0.08}$ at the 1σ confidence level in the model of $w_z = w_0 + w_1\, z$, $w_0 = -1.12^{+0.32}_{-0.30}$ and $w_1 = 1.90^{+2.10}_{-1.75}$ (at the 1σ confidence level) with $z_{\mathrm{T}} = 0.49^{+0.07}_{-0.09}$ in the model of $w_z = w_0 + w_1 z/(1+z)$, and $w_0 = -1.00^{+0.22}_{-0.25}$ and $w_1 = 0.54^{+0.85}_{-1.20}$ with $z_{\mathrm{T}} = 0.37^{+0.10}_{-0.07}$ at the 1σ confidence level in the model of $w_z = w_0 + w_1 z/(1+z)^2$. The contours are tighter than those only by using the SN Ia data. From these figures, a clear trend can be seen.

GRBs appear to be natural events when studying the Universe at very high redshifts. They can bridge the gap between the nearby SNe Ia and the CMB. GRBs establish a new insight to the cosmic acceleration. However, the density of the circumburst medium and the efficiency of conversion of the explosion energy to gamma-rays should be assumed in the Ghirlanda relation. This is naturally overcome in the Liang & Zhang relation.

Since the empirical relation of Liang & Zhang (2005) is cosmology-dependent, we use a strategy through weighing this relation in all possible cosmological models. We find that the transition redshift varies from $0.37^{+0.10}_{-0.07}$ to $0.69^{+0.05}_{-0.06}$. Although our constraints from the GRB sample are weaker than those from SNe Ia, the constraints from the GRB and SN Ia sample are more stringent than those from the SN Ia sample. A low-z GRB sample is needed to calibrate the relation in a cosmology-independent way. The MIDEX-class mission, which would obtain $>$800 bursts in the redshift range $0.1 \leqslant z \leqslant 10$ during a 2-yr mission (Lamb et al. 2005), will be dedicated to using GRBs to constrain the properties of dark energy. This burst sample would enable both Ω_{M} and w_0 to be determined to ± 0.07 and ± 0.06 (68 per cent confidence level), respectively, and w_1 to be significantly constrained. Probing the properties of dark energy by using GRBs is complementary (in the sense of parameter degeneracies) to other probes, such as CMB anisotropies and X-ray clusters (Lamb et al. 2005). New constraints from GRBs detected in the future would improve the study of cosmology.

ACKNOWLEDGMENTS

We thank Enwei Liang and Bing Zhang for helpful discussions, and the referee for valuable suggestions. This work was supported by the National Natural Science Foundation of China (grants 10233010 and 10221001).

REFERENCES

Amati L., 2004, Chin. J. Astron. Astrophys., 3, 455
Amati L. et al., 2002, A&A, 390, 81
Barth A. J. et al., 2003, ApJ, 584, L47
Bennett C. L. et al., 2003, ApJS, 148, 97
Bloom J. S., Frail D. A., Sari R., 2001, AJ, 121, 2879
Bloom J. S., Morrell N., Mohanty S., 2003, GCN 2212
Bloom J. S., Van Dokkum P. G., Bailyn C. D., Burton M. M., Kulkarni S. R., Schmidt B. P., 2004, AJ, 127, 252
Blustin A. J. et al., 2006, ApJ, 637, 901
Bromm V., Loeb A., 2002, ApJ, 575, 111
Butler N. R., Ricker G. R., Ford P. G., Vanderspek R. K., Marshall H. L., Jernigan J. G., Garmire G. D., Lamb D. Q., 2005, ApJ, 629, 908
Carroll S. M., Press W. H., Turner E. L., 1992, ARA&A, 30, 499
Chevallier M., Polarski D., 2001, Int. J. Mod. Phys. D, 10, 213
Ciardi B., Loeb A., 2000, ApJ, 540, 687
Dai Z. G., Liang E. W., Xu D., 2004, ApJ, 612, L101
Di Girolamo T., Riccardo C., Mario V., Di Sciasco G., 2005, J. Cosmol. Astropart. Phys., 4, 008
Djorgovski S. G., Kulkarni S. G., Bloom J. S., Goodrich R., Frail D. A., Piro L., Palazzi E., 1998, ApJ, 508, L17
Djorgovski S. G., Goodrich R., Kulkarni S. R., Bloom J. S., Dierks A., Harrison F., Frail D. A., 1999, GCN, 510
Firmani C., Ghisellini G., Ghirlanda G., Avila-Reese V., 2005, MNRAS, 360, L1
Friedmann A. S., Bloom J. S., 2005, ApJ, 627, 1
Ghirlanda G., Ghisellini G., Lazzati D., Firmani C., 2004a, ApJ, 613, L13
Ghirlanda G., Ghisellini G., Lazzati D., 2004b, ApJ, 616, 331
Ghirlanda G., Ghisellini G., Firmani C., Nava L., Tavecchio F., Lazzati D., 2005, A&A, submitted (astro-ph/0511559)
Godet O. et al., 2005, GCN 3222
Gou L. J., Mészáros P., Abel T., Zhang B., 2004, ApJ, 604, 508
Greiner J., Deimbert M., Estaban C., Kaufer A., Jaunsen A., Smoke J., Klose S., Reimer O., 2003, GCN 2020
Haislip J. et al., 2005, Nat, submitted (astro-ph/0509660)
Hjorth J. et al., 2003, ApJ, 597, 699

Holland S. T. et al., 2002, AJ, 124, 639
Jassal H. K., Bagla J. S., Padmanabhan T., 2004, MNRAS, 356, L11
Jimenez R., Band D. L., Piran T., 2001, ApJ, 561, 171
Kawai N. et al., 2005, preprint (astro-ph/0512052)
Kulkarni S. R. et al., 1999, Nat, 398, 389
Lamb D. Q., Reichart D. E., 2000, ApJ, 536, 1
Lamb D. Q. et al., 2005, preprint (astro-ph/0507362)
Liang E. W., Zhang B., 2005, ApJ, 633, 611
Liang E. W., Zhang B., 2006, MNRAS, submitted (astro-ph/0512177)
Linder E. V., 2003, Phys. Rev. Lett., 90, 091 301
Linder E. V., Huterer D., 2003, Phys. Rev. D, 67, 081 303
Maor I., Brustein R., Steinhardt P. J., 2001, Phys. Rev. Lett., 87, 049 901
Martini P., Garnavich P., Stanek K. Z., 2003, GCN 1980
Mészáros P., 2002, ARA&A, 40, 137
Möller P. et al., 2002, A&A, 396, L21
Mortsell E., Sollerman J., 2005, J. Cosmol. Astropart. Phys., 0506, 009
Perlmutter S. et al., 1999, ApJ, 517, 565
Phillips M. M., 1993, ApJ, 413, L105
Piran T., 1999, Phys. Rep., 314, 575
Piran T., 2004, Rev. Mod. Phys., 76, 1143
Price P. A. et al., 2003, ApJ, 589, 838
Riess A. G. et al., 1998, AJ, 116, 1009
Riess A. G. et al., 2004, ApJ, 607, 665
Sakamoto T. et al., 2005a, ApJ, 629, 311
Schaefer B. E., 2003, ApJ, 583, L67
Spergel D. N. et al., 2003, ApJS, 148, 175
Stanek K. Z. et al., 2005, ApJ, 626, L5
Tegmark M. et al., 2004, ApJ, 606, 702
van Paradijs J., Kouveliotou C., Wijers R., 2000, ARA&A, 38, 379
Vreeswijk P. M. et al., 2001, ApJ, 546, 672
Vreeswijk P., Fruchter A., Hjorth J., Kouveliotou C., 2003, GCN 1785
Weidinger M., Hjorth J., Gorosabel J., Klose S., Tanvir N., 2003, GCN 2215
Weller J., Albrecht A., 2001, Phys. Rev. Lett., 86, 1939
Weller J., Albrecht A., 2002, Phys. Rev. D, 65, 103 512
Xu D., Dai Z. G., Liang E. W., 2005, ApJ, 633, 603
Zhang B., Mészáros P., 2004, Int. J. Mod. Phys. A, 19, 2385

This paper has been typeset from a TEX/LATEX file prepared by the author.